Electrothermomigration-Induced Failure in Power IC Metallization

H. V. Nguyen[a], C. Salm[a], B. Krabbenborg[b], J. Bisschop[b], A. J. Mouthaan[a], F. G. Kuper[a,b]
[a] MESA+ Research Institute, University of Twente, Enschede The Netherlands
[b] Philips Semiconductors, Nijmegen, The Netherlands
P.O. Box. 217, 7500 AE Enschede The Netherlands
Phone: +31 (0) 53 - 489 4394 Fax: +31 (0) 53 - 489 2799
E-mail: H.V.Nguyen@el.utwente.nl

Abstract— **Metal migration by driving force of electron-flow and temperature gradient is a major reliability concern in power integrated circuits, especially for advanced integrated circuits where there are increasing density of the integrated power components and power dissipation. In this paper, we present a study of the combined effects of electromigration and thermomigration. A special test chip is designed for this study, in which several on-chip heater elements and temperature sensor are realized to impose and measure a temperature gradient, respectively. Our experimental results show that the electromigration lifetimes are much shorter in the presence of a temperature gradient than in a uniform temperature. The shortening of the electromigration lifetimes can be attributed to the effect of temperature gradient on electromigration-induced failure, rather than an additional driving force by thermomigration (due to a temperature gradient). Our observation is in qualitative agreement with recent theoretical model.**

Keywords— **Temperature gradient, Metallization, Power IC, Electromigration, Thermomigration.**

I. INTRODUCTION

The most common failures in metallic interconnects are related to electromigration (EM), which is the mass transport of a metal due to the momentum transfer between conducting electrons and metal atoms. EM causes failures in microelectronic components by creating voids, which eventually cause open circuits, and hillocks, which can cause short circuits. As device features reduce in ultra-large-scale integrated circuits, current densities increase with the metallization layer complexity. These issues make understanding EM-induced failure essential to design more reliable circuits. However, besides the EM-induced, the metallization used in power integrated circuit (IC) is also related to the thermomigration (TM)-induced because a high dissipation occurs in the underlying silicon where the active power elements are located and this can cause a significant temperature gradient. Furthermore, a high current density in the metal line can also cause a temperature gradient due to a non-uniform Joule heating. Eventually, a high temperature gradient can enhance EM [1] and induce TM [2]. Apparently, the magnitude of TM flux is usually much smaller than EM so that the role of TM in EM has not attracted much attention in almost all previous works. Recently, Ru [3] has reported that TM is the leading driving force for instability of the EM-induced mass transport in interconnect lines, and it plays a significant role in the EM failure of interconnect lines. This theoretical prediction seems to qualitatively agree with a previous experimental study [4]. In practice, the metal lines used in power IC are used to connect to the output and power devices that are characterized by large dimensions: the width and the thickness are normally several micrometers. Wider metal lines are already more susceptible to EM than narrow ones [5]. This is due to the near-bamboo microstructure (triple point) in the wider metal line having more flux divergences that the bamboo microstructure in the narrow line. Therefore, a combination of EM and TM would result in a serious reliability problem in metallization of power IC. A full understanding the role of TM in the EM-induced failure is very important for the design rule of power IC. Unfortunately, there is very limited experimental data in this area. In this paper, we will present a study into combined effects of EM and TM.

II. EXPERIMENTAL DETAILS

A. *Test structure descriptions*

The test structure, schematically shown in Fig. 1, has been designed with a conventional single metal level for

a standard EM testing [6]. Besides, it contains three heater elements and four temperature sensors.

The temperature sensors are p/n diodes, jus below the die surface, which are isolated by 0.5μm SiO_2. The heater elements are poly-Si lines. They were realized on three positions as shown in Fig. 1 (near cathode, anode, and in the middle of the metal line, respectively).

Fig. 1. *Schematic diagram of the test structure; TS is temperature sensor (intergraded diode); HE is heater element (poly-Si line); the showing dimensions are all in μm.*

Fig. 2. *SEM images: (a) the position to make cross-section; (b) the cross-section by FIB showing the different layers.*

Between the heater elements, there are two diodes, and the other two diodes are located at short distance to the heater elements to measure temperature gradient. Before deposition of the metal layers, the die surface is isolated by a 0.4μm SiO_2 layer, which is deposited by LPCVD (Low Pressure Chemical Vapor Deposition) using TEOS (Tetraethylorthosilicate). The aim of the use of TEOS is to improve the step coverage of the metal line over the poly-Si lines (heater elements). At the end, Si_3N_4 passivation layer with the thickness of 1.8μm was deposited by PECVD (Plasma Enhanced Chemical Vapor Deposition). Fig. 2 shows the cross-section made by FIB at the edge of poly-Si line to view the step coverage of the metal line and stack of layers of test structure.

A standard Al alloys AlSi(1%)Cu(0.04%) metallization was used in this test structure. The metal line was processed following the process manual of power metallization at a fab. The thickness and the width are 2.5μm and 10μm, respectively. The length of the metal line and the positions of heater elements and temperature sensors can be found in Fig. 1. The test structure was mounted in 24 pins ceramic package.

B. Experimental test set up

The test set up as shown in Fig. 3 has been employed for testing. The block (I) is a DC current source to force a constant current though heater elements to generate a temperature gradient. The block (II) is used for EM measurement. In this work, we have used a SourceMeter Keithley 2420.

Fig. 3. *The set up used in this work: block (I) is a current source connected to heater elements; (II) is a sourcemeter for electromigration test; (III) is the precision semiconductor parameter analyzer for the temperature measurements.*

It can be used to force a current from 500pA to 3A with a high stability, and the voltage is measured with an accuracy of 5-1/2 digit resolution [7]. These are matched with the standard as proposed in [6].

The block (III) is a scheme to measure the temperature inside the chip from the on-chip temperature sensor (integrated diode) and the package temperature from an external temperature sensor Pt100 on cap of the package, using a HP4156A semiconductor parameter analyzer. Different channels of HP4156A have been used such as SMU (source/monitor unit) and VMU (voltage monitor unit) as can be seen in Fig. 3. In this experiment, a Heraeus Intruments oven with a Shimaden Co. LTD. FP21 Series programmable controller is used. It can keep the temperature stable within tenths of a degree.

C. Diode temperature sensor calibrations

As reported in a pervious paper [8], the diode can be used as a temperature sensor. Equations to calculate the temperatures base on the Shocklely's relation as follows:

$$V_F = \frac{E_g}{q} + \frac{kT}{q}(\ln I_F - \ln K - r\ln T) \quad (1)$$

Where V_F and I_F are forward voltage and current of a diode, respectively, k is the Boltzamann's constant, T is the temperature, K, r, E_g are independent temperature constants. This relation shows that at a constant current, the forward voltage is almost a linear function of temperature and can be expressed as

$$T=A+BV \quad (2)$$

or a more accurate can be used higher order polynomials of the form:

$$T=A+BV+CV2 + \ldots \quad (3)$$

The constant A, B, and C are determined by the calibration over the temperature range at a constant current. Here, the temperature may be in degrees C.

Apparently, the Shocklely relation is only valid in the liner portions of the diode characteristic. Therefore, the diode characteristic needs to be measured at different temperatures to find a correct current to operate the diode during the calibration and the measurement. The calibration steps are conducted in an oven because it is easy to set and control the temperature. During a calibration step, the temperature of the oven is monitored from the temperature senor Pt100 mounted on the top center of the package. At the same time, the diode voltage is also monitored. At steady state (showed a variation of about 0.1°C on the temperature sensor Pt100), the diode voltage and the temperature indicated by the Pt100 were recorded. Next, the oven was set to a higher temperature, and the measurements were repeated as above.

D. The test procedures and conditions.

Conventional EM tests were performed at temperature T=202°C, and under different current density J=8, 10, and 12mA/μm^2. Other EM tests were also done at the same current densities but in the presence of a temperature gradient. The temperature gradient conditioning is done as follows; first, the oven temperature is set at 152°C, then heater element is used to locally heat up the metal line; the temperatures at heater elements are measured by on-chip temperature sensor and controlled at temperature of 202°C. This means that only the temperatures at the three heater elements reach at 202°C and the temperatures at the other locations is properly lower than 202°C. When the temperature is stable, the EM test is started.

EM test was also performed under different temperature gradient conditions at the same current density J=10mA/μm^2. The different temperature gradient conditions are done as follows; the oven temperatures (T_{oven}) are set at 127, 152, and 177°C, and then the temperatures at heater elements are controlled so that they are all at 202°C. This means the different temperatures between oven and heater element ($\Delta T_{max}=T_{HE}-T_{oven}$) are 25, 50, and 75°C. It should be mentioned that T_{oven} is measured before the local heating. Because the package of the chip is also heated up during locally heating, and the temperature measured on the cap of the package by Pt100 temperature sensor has a higher value. This temperature is considered as the ambient temperature of the chip (T_{amb}) during a temperature gradient conditioning. T_{amb} is always lower than the real temperature in the metal line due to an existent distance between the cap of the package and the chip surface. To represent the temperature of the metal line in case of the temperature gradient, the average temperature (T_{avg}), which is calculated by mean of the four temperatures measured from the four on-chip temperature sensors, is used. This average temperature was found quite comparable with the real temperature of the metal line that is determined by measuring the resistance in the presence of a temperature gradient, which can lead to an error due to the degradation of the metal line.

Throughout this paper, the time at which $\Delta R/R_0$= 15% was used as the failure criterion.

III. RESULTS AND DISCUSSIONS

A. *The temperature sensor calibration results*

The diode characteristics measured at different temperature are shown in Fig. 4. As can be seen, a current of 10µA is a perfect value to operate the diode in the liner portion for temperature measurement. The results of the calibrations at the room temperature and over a temperature range from 94 °C to 212°C are shown in Fig. 5. It also shows the linear and 2nd fits to the data. The standard deviations of liner and 2nd fits were observed about 0.7 and 0.1, respectively.

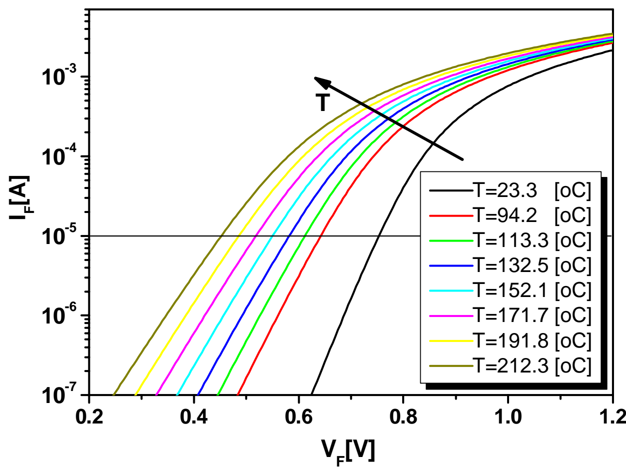

Fig. 4. *The diode characteristic I_F-V_F measured at different temperatures.*

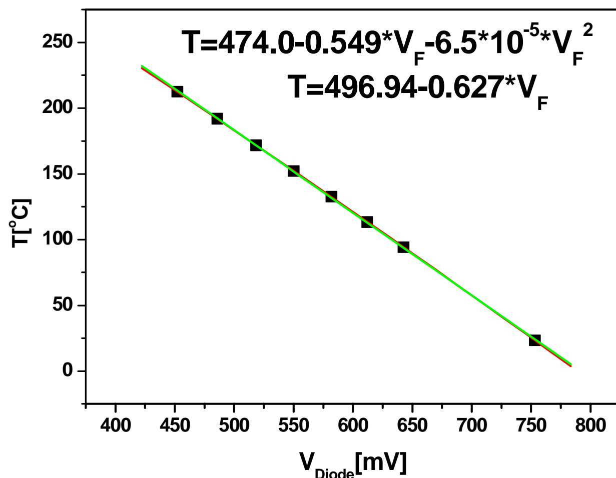

Fig. 5. *Calibration data for the diode (at 10µA current) fitted to a liner and 2nd order curves.*

B. *Electrothermomigration tests under different current densities*

The results of the relative resistance change (RRC) versus time observed from the EM tests at uniform temperature and in the presence of a temperature gradient are shown Fig. 6 (a) and (b), respectively. The current densities J=8, 10, 12mA/µm^2 were used in these tests. It can be seen that in both cases, a higher current density results in a higher rate of resistance increase of the metal line. Interestingly, the resistances increase faster in the presence of a temperature gradient than in the uniform temperature. The results of time-to-failure (TTF) is extracted from the RRC curves, are shown in the table I. It can be seen that the EM lifetimes are always shorter in the presence of a temperature gradient than in the uniform temperature. As mentioned above in these experiments, the stress temperature is strictly controlled. In the case of imposing a temperature gradient, the heater element is used to locally impose a temperature of 202°C. The temperatures at different locations are measured as shown in Fig. 7.

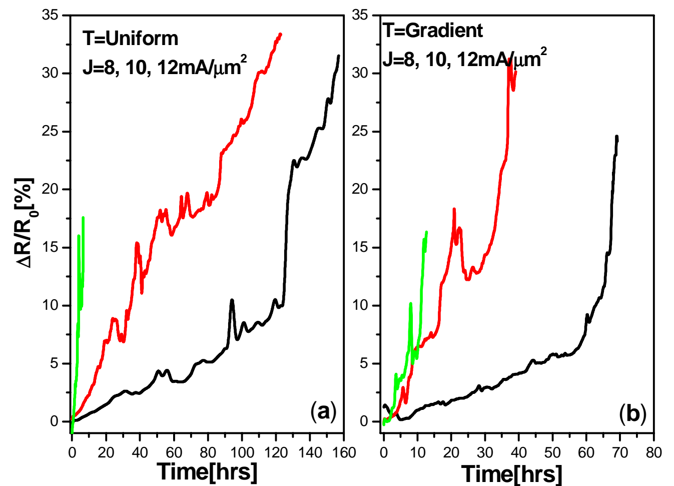

Fig. 6. *Relative resistance change under different EM test condition: (a) is the test results at constant temperature; (b) is the test results at temperature gradient.*

It can be seen that only at the locations near the heater elements reach the temperature of 202°C. The other locations are at temperature lower than 202°C so that the average temperature of the metal line is properly lower than 202°C. This is to indicate that the temperature gradient enhanced EM is not due to the cause of any higher temperatures. The temperature gradient (∇T) in this case is estimated about 0.067°C/µm (see Fig. 7).

A temperature gradient can cause TM (atoms diffuse from the hot to cold locations). It has been reported in

the literature [2] that TM can enhance the electromigration lifetime when the driving force sign of temperature gradient is the same as the driving force of the electron current. On the contrary, TM can improve the EM lifetime. In our experiment, there is no polarization of the temperature (hot to cool from cathode to anode, or the other way around). There are just few hot locations in the middle of the metal line. We always observe that the EM lifetimes in case of a temperature gradient are much lower than in case of a uniform temperature.

TABLE I. TTF RESULTS UNDER UNIFORM AND GADIENT TEMPERATURES

J[mA/μm²]	TTF [hrs] Temp. Uniform	TTF [hrs] Temp. Gradient
8	125.8	67.1
10	46.6	19.8
12	11.8	3.9

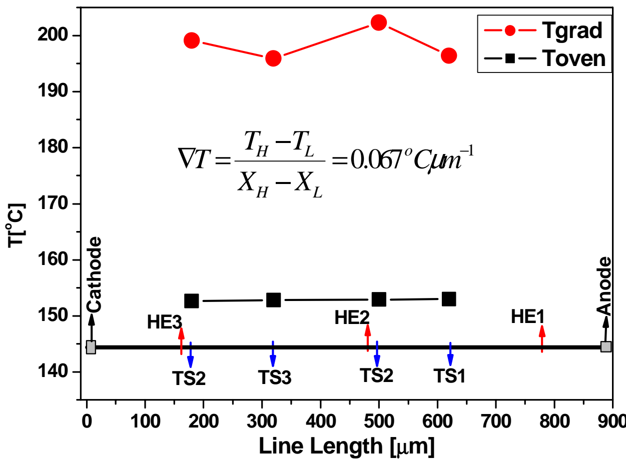

Fig. 7. *The temperatures measured by the temperature sensor (TS) at near heater element (HE) before and after the geneartion of temperature gradient.*

The reductions are almost 50% for all cases under different current densities (J=8, 10, 12 mA/μm²). It can be seen that the temperature gradient (∇T) is not yet too high but it strongly affects the EM lifetime. Therefore, we can deduce that TM plays a significant role in the EM-induced failure. This is in qualitative agreement with recent theoretical model in [3]. A mode to explain our experimental observation will be discussed further in the next section.

It has been recognized that the Joule heating during EM testing can also result in a temperature gradient itself that can result EM failure with different failure mechanism [9]. With this in mind, the Joule heating needs to be estimated for our experiment. To do so, the resistance of the metal line was measured at different temperatures to find its thermal resistance coefficient. Fig. 8 presents a plot of resistance versus temperature. Taking equation

$$R = R(T_{ref}) + S(T - T_{ref}) \quad (4)$$

where S is slope of the resistance versus temperature plot and $R(T_{ref})$ is the resistance of the test line at a reference temperature T_{ref}. We found the slope S= $6.1\times10^{-3}/^oC$.

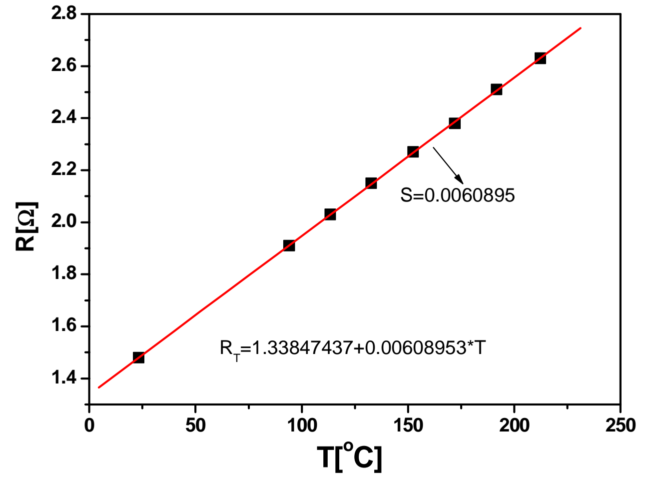

Fig. 8. *Resistance versus temperature for metal line of the test structure.*

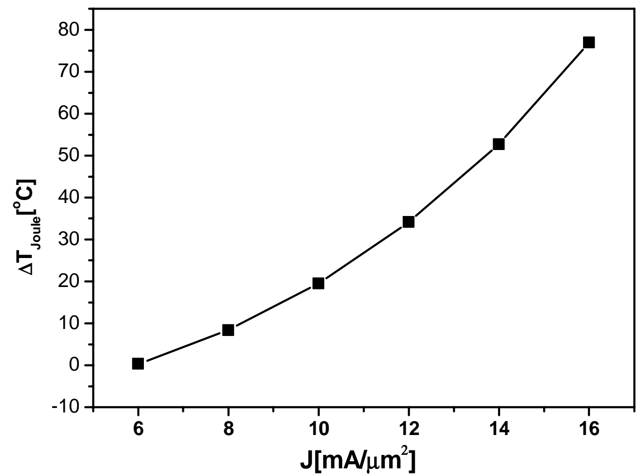

Fig. 9. *The temperature increases due to the Joule heating.*

The Joule heating can be calculated by equation as follows [6];

$$\Delta T_{Joule} = \frac{R_H - R(T_H)}{S} \quad (5)$$

Where $R_H(T_H)$ is the resistance measured at stress temperature T_H with a low current, and R_H is resistance measured at stress temperature and stress current (for EM tests). In Fig. 9, we plot ΔT_{joule} versus current density for the test structure held at an oven temperature of 152°C with current densities ranging from 6 to 16mA/μm.

It is well known that MTF for EM follows the Black equation [10]

$$MTF = Aj^{-n} \exp\left(\frac{E_a}{kT}\right) \quad (6)$$

Where, j is the current density, E_a is the activation energy, n and A are constant, and k is Boltzman's constant, T is the temperature in Kelvin degrees. With connection, Fig. 10 shows the ln(TTF) versus ln(J) for the test results with different current density and both temperature conditions (uniform and gradient temperature). To find the value of n, the linear fitting of TTF data to different current density is made. The calculated n values are about 5.8 and 7.0 for uniform and gradient temperatures, respectively (see Fig. 10).

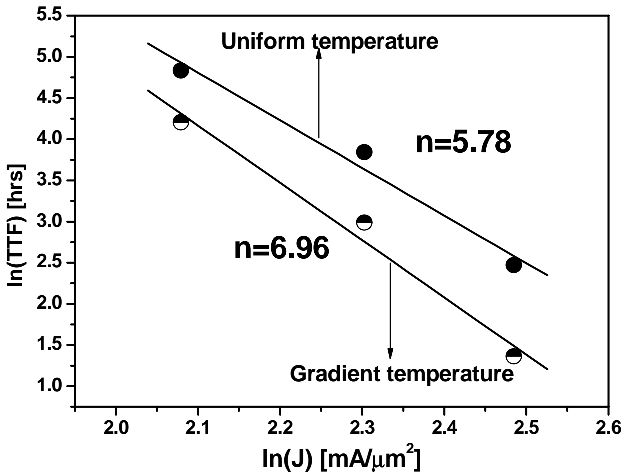

Fig. 10. *Fitting of TTF data at three different current densities for both temperature conditions.*

These n values are much larger than reported by other authors (from 1.0 to 3.0) [10][11]. The reason is that the Joule heating under our experimental current density is too high to be ignored, and T in equation (6) represents the actual temperature in the metal line. Therefore, the Joule heating ΔT_{Joule} must be added in the equation (6). Then equation (6) becomes

$$MTF = AJ^{-n} \exp\left(\frac{Ea}{k[T + \Delta T_{Joule}]}\right) \quad (7)$$

In Fig. 11, we plot ln(TTF)-Ea/k(T+ΔT_{Joule}) versus ln(J), and the linear fit results are shown in the same figure. It can be seen that to make the Joule heating correction, the E_a value needs to be estimated in advance. As mentioned above, the metal line used in this test structure was fabricated with a standard process at a fab following a design manual. Therefore, we took the E_a value of 0.65eV from the design manual for the correction. Another thing to mention is that in case of temperature gradient, the average temperature is used to represent the metal line temperature to make the correction.

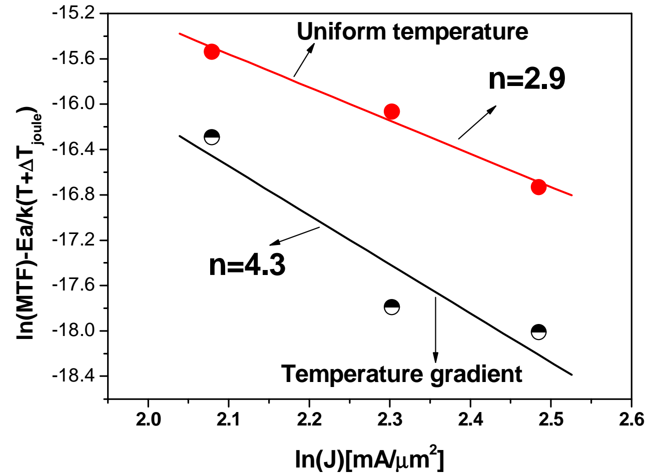

Fig. 11. *Fitting of TTF data with the correction of Joule heating at three different current densities for both temperature conditions.*

The calculated n values after the Joule heating correction are 2.9 and 4.3 for the EM tests with uniform temperature and temperature gradient, respectively. It can be seen that the n value in case of uniform temperature is an acceptable value and comparable with reported values in literature as well as with the value of process manual (n=2.3). However, the n value in case of temperature gradient is still too high. This indicates that there is an interaction of temperature gradient on the EM-induced, and the activation energy E_a from design manual cannot be used for the joule heating correction, or the Black equation may not be suitable for the combination of TM and EM, and it needs some kind of modifications due to the effect of TM. However, this is not yet complete understand from this study.

C. Electrothermomigration tests under different temperature gradient conditions

Fig. 12 shows the temperature gradient conditions measured by the on-chip temperature sensor for the

different ΔT_{max} conditions (T_{oven}=177, 152, and 127°C and T_{HE}=202°C). The estimations of ∇T values are shown in table II. RRC results of the EM tests with stress current density of 10mA/μm^2 under these temperature gradient conditions are shown in Fig. 13.

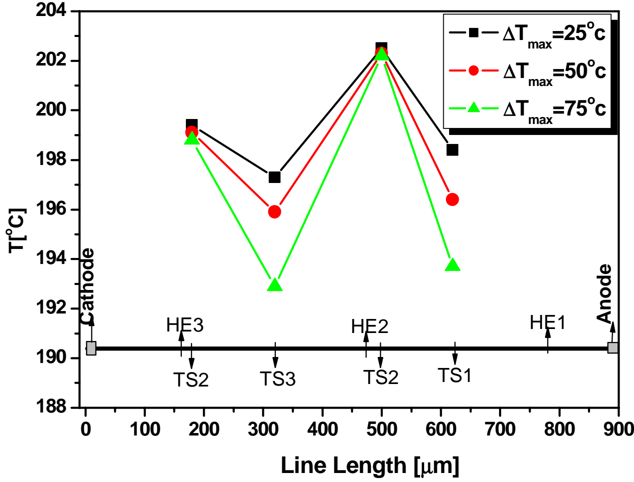

Fig. 12. *The temperatures measured by the temperature sensor (TS) at different locations from different temperature gradient conditions.*

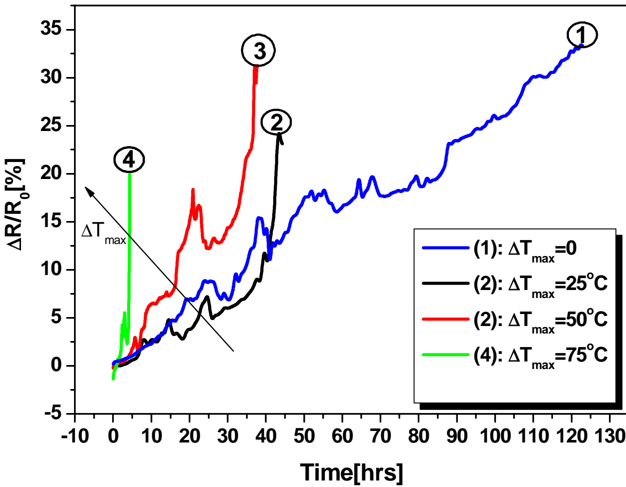

Fig. 13. *RRC results of EM tests under current density of 10mA/μm^2 and at different temperature gradient conditions.*

TABLE II. TTF RESULTS UNDER DIFFERENT TEMPERATURE GRADIENT CONDITIONS.

T_{HE}-T_{oven}[°C]	0	25	50	75
∇T [°C/μm]	0	0.041	0.067	0.10
T_{oven}[°C]	202	177	152	127
TTF[hrs]	46.6	41.8	19.8	4.3

It can be seen that the increase of ∇T results in a high rate of RRC increase. This means the EM lifetimes are decreased. The results of TTFs are extracted and shown in table II. It is observed that the acceleration factor of ∇T for the EM lifetime is not uniform as can be seen as the calculations below:

(∇T1/∇T2) = 0.61 => AF1 (TTF1/TTF2) = 2.1

(∇T2/∇T3) = 0.67 => AF2 (TTF2/TTF3) = 4.5

This can deduced that one single acceleration factor could not be used to make an extrapolation of the EM lifetime under the presences of other temperature gradient conditions.

D. Failure mechanism discussion

It is well accepted that the EM failure is caused by vacancy mechanisms. There are typically three primary driving forces for vacancy diffusion in the metal line under an applied current; (i) the electrical current (electromigration), (ii) mechanical stress (stressmigration) gradient, (iii) temperature gradient (thermomigration). Based on the model proposed by Clement and Thompson [12], a vacancy flux can be approximated by the following equation:

$$J_v = -D_v\left[\nabla C_v + \frac{C_v}{kT}\left(Z^* e\rho j + \Omega\nabla\sigma - \frac{Q^*}{T}\nabla T\right)\right] \quad (8)$$

Where D_v is the vacancy diffusivity, kT is the thermal energy, Z^* is the effective change number, e is the elementary charge, ρ is the resistivity, j is the current density, Ω is the atomic volume, ∇ is the gradient operator, σ is the tensile stress, and Q* is the coefficient of heat flux. As mentioned above, TM has been ignored in recent research, due to the fact that the EM driving force is much larger the TM driving force. Now, we estimate both of these driving forces in our case for a comparison. In these calculations, some parameters are taken from literature: Q*=1eV, ∇T=0.067 °C/μm (our experiment), j=10mA/μm^2, Z*=-10, T=[202+273]K (our experiment), ρ=4μΩcm, we find; the TM driving force F_{TM} = Q*(∇T/T) ≈ 1.4eV/cm, and the EM driving force F_{EM}=Z*eρj=40eV/cm. These calculations are to point out that the driving force of TM is much smaller than that of EM. Therefore, the reduction of the EM lifetime can not explained due to an enhancement of TM. In early studies [1][13], they have shown that besides the small TM flux, the temperature gradient induces flux divergences [13]. Therefore, the EM-induced under the temperature gradient can occur with two mechanisms as follows; (i) the flux divergence due to the microstructure (grain boundary) and (ii) the flux divergence due to the temperature gradient. With a high temperature gradient

in the metal line, the second mechanism can be a dominated mechanism, and the failure location is typically near to the location of maximum temperature gradient, but not exactly at the highest temperature location. Because the failure locations are determined by the gradient of atom flux rather than the magnitude of atom flux. With EM under a uniform temperature, the flux divergence due the microstructure is dominated so that the failure locations are randomly distributed. Microscopic verifications the failure locations of our samples are shown Fig. 14 (a) and (b) for uniform temperature and temperatures gradient, respectively.

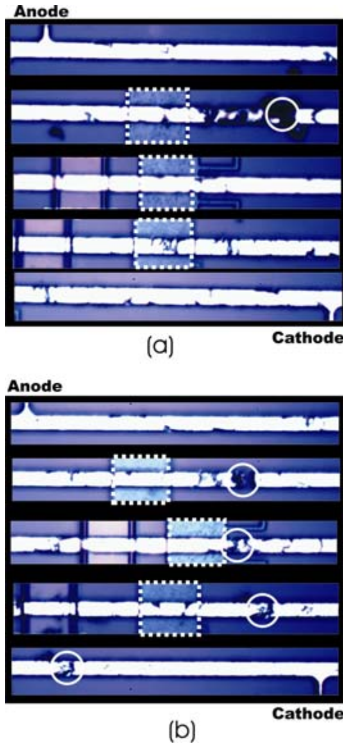

Fig. 14. *Failure locations by EM tests with J=12mA/µm: (a) in a uniform temperature, (b) in the presence of a temperature gradient.*

We observed that mostly, the failure locations by the EM-induced under the temperature gradient distribute near the hottest region and on the cathode side heater elements (heater element regions are square symbols). This can be understood with the model as shown in Fig. 15. From equation (8), it can be seen that the atom flux (or vacancy flux) is exponentially proportional to the temperature by the relation: $J_v(-J_{Atom})\sim D_o Exp(-E_a/kT)$. Therefore, the atom flux at the highest temperature location is much higher that than the other locations (see Fig. 15), this results in a high gradient of atom flux somewhere near the heater element but not at the heater element. It means that the highest flux divergences are somewhere near heater elements, where the failure locations are to be. This model agrees well with the failure locations that we have observed.

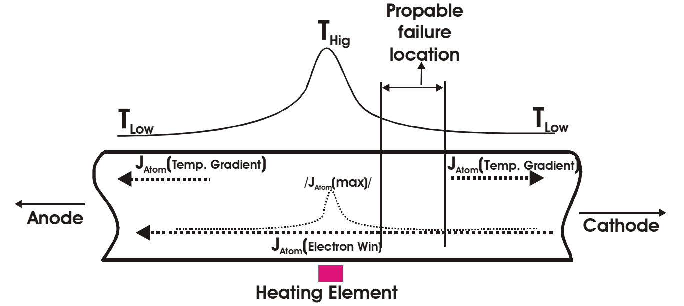

Fig. 15. *A model for failure locations in case of EM test under a temperature gradient.*

The discussion above is just a qualitative explanation to understand the effect of the temperature gradient on EM. Recently, Ru has developed a physical model, in which the important parameters such as C_v, T, j and σ are treated under perturbed state in the present of a temperature gradient, to analyses the effect of temperature gradient on the EM-induced failure.

It is well know that the continuity equation proposed in [14] is popularly used to model the EM phenomena of a conductor line. It is expressed as follows;

$$\frac{\partial C_v}{\partial t} - \frac{\partial C_L}{\partial t} = -\nabla J_v \qquad (9)$$

Where, C_L is the concentration of lattice sites.

One the equation (8) is applied for the continuity equation. The parameters in equation (8) must be treated as perturbed states as follows [3];

$$C_v = C_v^o + \Delta C_v(x,t); \qquad j_v = j_v^o + \Delta j_v(x,t)$$
$$\sigma_v = \sigma_v^o + \Delta\sigma_v(x,t); \qquad C_L = C_L^o + \Delta C_L(x,t)$$
$$T = T^o + \Delta T(x,t) \qquad (10)$$

Here the superscript "0" denotes as the unperturbed state, and Δ denotes the variations. The other parameters are also under a relatively perturbed state to be D (diffusion coefficient) and ρ (resistivity of the conductor line). They are dependent on the temperatures as expressed below:

$$D = D^* \exp(E_a/kT)\ ; \quad \rho = \rho_0\,[1 + \alpha(T - T_{ref})]\ (\alpha > 0) \qquad (11)$$

Where, D^* is the material constant, T_{ref} is the reference temperature, and α is a thermal resistance coefficient.

Ru [3] has carried out an analytically solving equation

(9), using equations (8), (10), and (11). Ru's[3] result suggested that temperature gradient plays a significant role in the EM-induced failure. This is consistent with our experimental results.

IV. CONCLUSIONS

We have presented an experimental study into electrothermomigration. A special test structure has been designed and fabricated which allows temperature gradient to be locally imposed and measured along the metal line.

The electromigration lifetimes in the presence of a temperature gradient are much shorter than that in a uniform temperature, in which the uniform temperature is kept the same value as the peak temperature in the temperature gradient. Results show that both electromigration tests in the presence of uniform temperature and temperature gradient are proportional to j^{-n}. With a correction for the Joule heating, the MTF and j are well fitted to the Black equation, and an acceptable n value has been found about 2.9 for uniform temperature test results. However, the fit is not good enough for the temperature gradient test results, and the observed n value of 4.3 is a bit too high compared with the literature.

Result also shows that a higher of temperature gradient results in a higher reduced rate of the electromigration lifetime, and non-uniform acceleration factor of temperature gradient for electromigration is observed.

The modeling of failure mechanism has shown that the reduction of the electromigration lifetimes in the presence of a temperature gradient is determined by the effect of temperature gradient on the electromigration-induced failure, rather than an additional driving force by thermomigration.

Eventually, our experimental observation has shown a significant role of temperature gradient in the electromigration-induced failure, which is in qualitative agreement with recent theoretical modeling [3].

V. ACKNOWLEDGEMENTS

This work is being supporting by the Dutch Foundation for Fundamental Research of Matter (FOM) and Philips Semiconductors, Nijmegen, The Netherlands.

VI. REFERENCES

[1] A.P. Schwarzenberger, C.A. Ross, J.E. Evetts, and A.L. Greer, "Electromigration in the presence of a temperature gradient: Experimental Study and Modelling", J. Electronic. Materials, Vol.17, No.6, 1988, p.473.

[2] G. Eeiling, L. Zhhigou, Z. Hong, Z. Wei, J.Y. S. Yunghua, and S. Guangdi, "Temperature gradient impact on electromigration failure in VLSI metallization", Proc. 14th IEEE-THERM Symp. 1998, p.122.

[3] C.Q. Ru, "Thermomigration as driving force for instability of electromigration induced mass transport in interconnect lines", J. Material Science, Vol. 35, 2000, p.5575.

[4] A.F. Bastawaros and S.K. Kim, "Experimental study on electric-current induced damage evolution at the crack tip in thin film conductor", Tran. ASME. J. Electron. Packaging, Vol.120, No. 4, 1998, p.354.

[5] I. De Munari, A. Scorzoni, F. Tamarri, D. Govoni, F. Corticelli and F. Fantini, " Drawbacks to using NIST electromigration test structures to test bamboo metal lines", IEEE Trans. Electon Devices, Vol. 41, No. 12, 1994, p.2280.

[6] A. Scorzoni, M. Impronta, I. De Munari, , and F. Fantini, "A proposal for a standard procedure for moderately accelerated electromigration tests on metal lines", Microelectron. Reliab. Vol. 39, 1999, p. 615.

[7] Keithley Model 2420 Series SourceMeter, User 's Manual.

[8] H.V. Nguyen, C. Salm, J. Vroemen, J.Voets, B. Krabbenborg, J. Bisschop, A.J. Mouthaan, and F.G. Kuper, "Fast thermal cycling stress and degradation in multiplayer interconnect Proc. of the 4th Annual Workshop on Semiconductors for Future Electronics, 2001, p.136.

[9] Z.H. Li, G.Y. Wu, Y.Y. Wang, Z.G. Li, Y.H. Sun, "Dependence of electromigration caused by different mechanisms on current densities in VLSI interconnects", J. Mater. Science. : Mater. In Electronics. Vol. 10, 1999, p. 653.

[10] J. R Black, "Electromigration – A brief survey and some recent results", IEEE Tran. Electron Devices, Vol. ED-16, No. 4, 1969, p. 338.

[11] Y.C. Joo and C.V. Thompson, "Electromigration-induced transgranular failure mechanisms in single-crystal aluminum interconnects", J. Appl. Phys. Vol. 81, No. 9, 1997, p. 6062.

[12] J.J. Clement, C.V. Thompson, " Modeling electromigration-induced stress evolution in confined metal line", J. Appl. Phys. Vol. 78, No. 2, 1995, p. 900.

[13] J.R. Lloyd, M. Shatzkes, and D.C. Challener, " Kinetic study of electromigration failure in Cr/Al-Cu Thin Film Conductors covered with polyimide and the problem of the stress dependant activation energy", Proc. Int. Rel. Phys. Sym., 1988, p. 219.

[14] M.A. Korhonen, P. Borgesen, K.N. Tu, Che-Yu li, " Stress evolusion due to electromigration in confined metal lines", J. App. Phys. Vol. 73, No. 8, 1993, p. 3790.